AAEC/E276

AAEC/E276

AUSTRALIAN ATOMIC ENERGY COMMISSION

RESEARCH ESTABLISHMENT
LUCAS HEIGHTS

THERMAL DECOMPOSITION OF AMMONIUM URANATES

by

G.H. PRICE

W.I. STUART

April 1973

ISBN 0 642 99555 9

AUSTRALIAN ATOMIC ENERGY COMMISSION

RESEARCH ESTABLISHMENT

LUCAS HEIGHTS

THERMAL DECOMPOSITION OF AMMONIUM URANATES

by

G.H. Price

W.I. Stuart

ABSTRACT

Thermal decomposition of ammonium uranates in various atmospheres was studied using thermogravimetric analysis, differential thermogravimetric analysis, differential thermal analysis and infra-red spectrophotometry. The various stages of decomposition are discussed in terms of reaction mechanisms. The effect of nitrate impurities on thermal decomposition is briefly described. It is concluded that the ammonium uranate system at equilibrium is a continuous non-stoichiometric system with zeolitic properties.

National Library of Australia card number and ISBN 0 642 99555 9

The following descriptors have been selected from the INIS Thesaurus to describe the subject content of this report for information retrieval purposes. For further details please refer to IAEA–INIS–12 (INIS: Manual for Indexing) and IAEA–INIS–13 (INIS: Thesaurus) published in Vienna by the International Atomic Energy Agency.

(0) INFRARED SPECTRA; PYROLYSIS; SPECTROPHOTOMETRY
(1) AIR; AMMONIUM COMPOUNDS; ARGON; CHEMICAL REACTION; KINETICS; DIFFERENTIAL THERMAL ANALYSIS; IMPURITIES; NITRATES; THERMAL GRAVIMETRIC ANALYSIS; URANATES
(2) HYDRATES; HYDROXIDES; URANYL COMPOUNDS

CONTENTS

CONTENTS (Cont'd)

1. INTRODUCTION

Uranium dioxide for nuclear fuel is commonly produced by heating ammonium uranate (AU) in hydrogen. Several stages of thermal decomposition precede the final reduction to UO_2 but apart from the work of Price (1971) on self-reduction, these have not been examined in much detail (Notz et al. 1960; Ippolitova et al. 1961; Woolfrey 1969).

This report describes an investigation in which thermal analysis, infra-red (i.r.) spectrophotometry and gas analysis were employed to study thermal decomposition of AU in various atmospheres. We took the following matters into account:

(i) AU is not a well-defined stoichiometric compound; its composition varies according to conditions of preparation.

(ii) Although conflicting views (Cordefunke 1962, 1970; Stuart and Whateley 1969) exist concerning the nature of AU, the balance of experimental evidence (see Appendix) indicates that the AU system is non-stoichiometric, represented by the molecular formula $UO_2(OH)_{2-x}(ONH_4)_x\ zH_2O$ where x is continuously variable in the limits $x = 0$ and $x = 0.7$.

(iii) AU products used for manufacture of UO_2 are generally obtained by precipitation from uranyl nitrate solution. The precipitates contain occluded nitrate as a major impurity, and compositions usually fall within limits corresponding to $x = 0.3$ and $x = 0.5$.

The results illustrate the major chemical stages in thermal decomposition of nitrate-free AU, and demonstrate the influence of nitrate impurities on thermal decomposition.

2. EXPERIMENTAL

2.1 Preparation of Samples

Uranium peroxide prepared free of nitrate (Dawson et al. 1956) was calcined in air at 470°C for 1 hour to form UO_3, which was then converted to uranyl hydroxide hydrate by exposure to water vapour for 3 days at room temperature.

$UO_2(OH)_2 \cdot H_2O$ was then converted to AU, either by absorption of ammonia from argon bubbled through ammonium hydroxide solution or by reaction with NH_4OH solution.

2.2 Thermoanalytical Measurements

Thermogravimetric (TG) measurements were made with a Cahn RG Electrobalance. An aluminium sample holder was used up to 500°C and a platinum holder was used at higher temperatures. (When platinum was used with AU in air, it catalysed the oxidation of ammonia gas evolved at 300°C, and a spurious exotherm in the differential thermal analysis (DTA) trace was similarly produced by platinum

thermocouples.)

The apparatus for DTA was designed to ensure a free flow of gas over the sample and rapid removal of gaseous decomposition products. The sample material and alumina reference were contained in shallow holes (10 mm dia. x 7 mm) in an aluminium block held in a horizontal silica tube (25 mm dia.).

2.3 Chemical Analysis

Ammonia gas evolved during decomposition was estimated by monitoring the effect of exit gases on the electrical conductivity of standardised solution of hydrochloric acid. Measurements were reproducible to within ± 2 per cent.

Total ammonia content of an AU sample was estimated by dissolving the solid in acid, making the solution alkaline and distilling to dryness into standardised HCl solution. The sodium phenate method (USAEC 1962) was also used in conjunction with a spectrophotometer. Results obtained by the two methods were comparable within their reproducibilities of ± 5 per cent.

Total uranium was determined gravimetrically by heating samples in air to 850°C to form U_3O_8. In addition U(VI) was measured by a volumetric method (Davies and Gray 1964). To determine U(IV), samples were dissolved in phosphoric acid; the solutions were then boiled to hydrolyse any pyrophosphate and then titrated with standard Ce(IV) solution.

2.4 Infra-red Spectrophotometry

Experimental techniques were essentially as described previously (Stuart and Whateley 1969). Infra-red spectra were recorded on Perkin-Elmer spectrophotometers model 21 and model 225, with samples in the form of Nujol mulls or thin films deposited on Irtran 2 plates.

3. RESULTS AND DISCUSSION

Before discussing thermal decomposition, it is first necessary to describe infra-red (i.r.) spectra of both ammonium uranate and the parent compound $UO_2(OH)_2 \cdot H_2O$.

3.1 Infra-red Spectrum of $UO_2(OH)_2 \cdot H_2O$

As shown in Figure 1a, $UO_2(OH)_2 \cdot H_2O$ displays four major regions of optical absorption (Stuart and Whateley 1969): a complex series of absorption bands between 3100 cm^{-1} and 3650 cm^{-1} is due to O-H stretching vibrations of hydroxyl groups and coordinated water molecules; the band at 1620 cm^{-1} arises from the vibrational bending mode, δH_2O, of water molecules; and the band at 955 cm^{-1} can be assigned to the asymmetric vibrational frequency ν_3 of the uranyl group. A band at 1000 cm^{-1} shifts to 720 cm^{-1} in the deuterium analogue $UO_2(OD)_2 \cdot D_2O$ and is therefore assigned to a bending deformation of hydroxyl groups.

3.2 Infra-red Spectra of Ammonium Uranates

Infra-red spectra of AU compounds, illustrated in Figures 1b, 2 and 3 have four additional features:

(i) Only two overlapping bands are observed at 3460 cm^{-1} and 3200 cm^{-1}. These arise from O-H and N-H stretching vibrations.

(ii) An absorption band at 1410 cm^{-1} is due to the vibrational bending mode of NH_4^+

(iii) As shown in Figure 2, frequency ν_3 of the uranyl group decreases continuously from 955 cm^{-1} for x=0 to about 890 cm^{-1} for x = 0.7.

(iv) The relative absorbance of δH_2O at 1620 cm^{-1} decreases as x increases (Figure 3); that is, the proportion of coordinated water molecules decreases with increasing NH_4^+ content.

3.3 Thermal Decomposition of $UO_2(OH)_2 \cdot H_2O$

Decomposition of $UO_2(OH)_2 \cdot H_2O$ in a non-reducing atmosphere occurs in three quite separate steps; these are described by thermoanalytical and i.r. data shown in Figures 4 and 5. The first endothermal process, with a differential peak at 140°C, involves removal of coordinated water molecules; after completion of the process the δH_2O band at 1620 cm^{-1} is no longer evident (Figure 5b). A single O-H band at 3350 cm^{-1} still remains and disappears only after heating to about 350°C (Figure 5c). Clearly the second process involves decomposition of anhydrous uranyl hydroxide. The third endothermal peak denotes formation of U_3O_8 from decomposition of UO_3.

3.4 Thermal Decomposition of Ammonium Uranate

Figures 6-9 show typical data for decomposition of AU in an inert atmosphere. There are four overlapping stages of decomposition, each involving a loss in weight (Figures 6 and 7). The four stages are listed in Table 1 together with peak temperatures and the approximate temperature range over which each occurs.

TABLE 1 - AU HEATED IN ARGON AT 5°C min^{-1}

Stage	Peak Temperature (°C)	Temperature Range (°C)	Remarks
I	80	20-120	Endothermal
II	160	120-200	"
III	275	200-350	"
IV	400	350-450	Exothermal

3.4.1 Stage I and Stage II: decomposition of AU

Our data do not reveal a clear chemical distinction between Stages I and II, but the two processes have certain common features as follows:

(i) No ammonia gas is released (Figure 7b). The δNH_4^+ band at 1410 cm^{-1} and the 3210 cm^{-1} band, which we attribute to the N-H stretching vibration, remain unaltered (Figure 9b).

(ii) With increasing temperature the 1620 cm^{-1} band diminishes progressively and is no longer evident after completion of Stage II at about 200°C (Figures 8 and 9). Thus coordinated H_2O molecules are removed from AU during both stages

It seems likely, therefore, that the transition from Stage I to Stage II is related to a structural change within the solid. It has been proposed (Stuart and Whateley 1969) that AU resembles lamellar clay material with H_2O molecules held between lamellae, and the structural analysis of Christ and Clark (1960) supports this view. Dehydration of clay minerals frequently occurs in several steps, each accompanied by structural change and a decrease in interlamellar spacing, as is found, for example, in the dehydration of vermiculite (Brown 1961).

Table 2 gives the amount of dehydration in the two stages for three AU products.

TABLE 2 - AU HEATED IN ARGON AT 5°C min^{-1} H_2O EVOLVED IN STAGES (I + II)

	Total H_2O Evolved (mole $mole^{-1}$)	Coordinated H_2O Molecules Removed (mole $mole^{-1}$)	H_2O Evolved by Dehydroxylation (mole $mole^{-1}$)
$UO_2(OH)_{1.69}(ONH_4)_{0.31} \cdot 0.86H_2O$	1.37	0.86	0.51
$UO_2(OH)_{1.61}(ONH_4)_{0.39} \cdot 0.64H_2O$	1.13	0.64	0.49
$UO_2(OH)_{1.52}(ONH_4)_{0.48} \cdot 0.43H_2O$	0.98	0.43	0.55

Because of overlap between stages, these figures are at best semi-quantitative but nevertheless they show that some dehydroxylation occurs below 200°C. At temperatures above 200°C the O-H stretching band at 3460 cm^{-1} is however still apparent at reduced intensity, indicating that a proportion of hydroxyl groups is retained through to Stage III.

3.4.2 Stage III: thermal decomposition of AU

NH_3 and H_2O are evolved simultaneously during the third stage (Figure 7).

Data for the release of NH_3 and H_2O are listed in Table 3.

TABLE 3 - AU HEATED IN ARGON AT $5^oC\ min^{-1}$: STAGE III

Initial AU Composition $x = NH_4^+:U$	H_2O Released (mole $mole^{-1}$)	NH_3 Released (mole $mole^{-1}$)	NH_3 Retained (mole $mole^{-1}$)
0.21	NA	0.07	0.14
0.31	0.50	0.18	0.13
0.39	0.50	0.21	0.17
0.38	NA	0.18	0.21
0.48	0.45	0.38	0.10
0.60	NA	0.43	0.17

NA : Data not available.

The amount of NH_3 released is less than one might expect from the composition of the original AU material. A portion of NH_3 is retained by the solid and is never released as NH_3 gas.

Figure 9 reveals a notable result that explains retention of NH_3 in the solid. During Stage III the δNH_4^+ band diminishes, and two additional bands can be observed at 1590 cm^{-1} and 1250 cm^{-1}; simultaneously, two sharp bands appear at 3310 cm^{-1} and 3230 cm^{-1} superimposed upon the broad OH band. Now, ammines such as $(Co(NH_3)_6)Cl_3$ have NH_3 deformation bands in the regions 1650 - 1560 cm^{-1} and 1350 - 1150 cm^{-1}, whereas ammonium salts absorb at 1410 cm^{-1}. We therefore attribute the three bands at 3310 cm^{-1}, 1590 cm^{-1} and 1250 cm^{-1} to an <u>ammoniate group</u> $H_3N\rightarrow$, and assign these bands to N-H stretching (3310 cm^{-1}), the degenerate asymmetric bending mode (1590 cm^{-1}) and the symmetric bending mode (1250 cm^{-1}) of coordinated $H_3N\rightarrow$ groups. The 3230 cm^{-1} band is assigned to the N-H stretching vibration of residual NH_4^+.

We can now visualise several group interactions that might occur in Stage III. These can be classed in two categories as follows:

<u>Class 1: Reactions involving hydroxyl groups</u>

$$2 - OH = -O- + H_2O\ (g) \qquad \ldots(1)$$

$$-OH + - ONH_4 = -O- + H_2O\ (g) + NH_3\ (g) \qquad \ldots(2)$$

$$-OH + - ONH_4 = -O- + H_2O\ (g) + H_3N\rightarrow \qquad \ldots(3)$$

<u>Class 2: Reactions of paired $-ONH_4$ groups</u>

$$2 - ONH_4 = -O- + H_2O\ (g) + 2NH_3\ (g) \qquad \ldots(4)$$

$$2 - ONH_4 = -O- + H_2O\ (g) + NH_3\ (g) + H_3N \rightarrow \quad \ldots(5)$$

$$2 - ONH_4 = -O- + H_2O\ (g) + 2H_3N \rightarrow \quad \ldots(6)$$

A qualitative assessment of these various reactions and their relative importance can be made by considering the DTA data, and particularly the ratio R = (rate of NH_3 release)/(rate of H_2O release). If class 1 reactions predominate (which certainly should be the case for the initial part of Stage III), then R must $\leqslant 1$, whereas class 2 reactions give $R \leqslant 2$. Figure 10 gives values of R as a function of temperature for three ammonium uranates. For two compounds ($x = 0.31$ and $x = 0.39$) the magnitude of R never exceeds about 0.5, which suggests that Stage III occurs by class 1 reactions. The third AU compound ($x = 0.48$) behaves differently, with R increasing to about 2.0 in the latter part of Stage III. This is as one might expect: as the magnitude of x increases, there is an increasing probability of interaction between neighbouring $-ONH_4$ groups.

3.4.3 Stage IV: Thermal decomposition of ammonium uranates

Stage IV, which has recently been described in some detail (Price 1971), is a process of self-reduction within the solid; it is not reduction of UO_3 by evolved NH_3 gas as proposed by Notz et al. (1960). The process is accompanied by a sharp decrease in the concentration of $H_3N \rightarrow$ although NH_3 gas is not evolved, and simultaneously the U(IV) concentration in the solid increases (Figure 11).

The solid residue after completion of Stage IV is U_3O_8: the measured ratio U(IV)/U(VI) is about 0.32 - 0.33 and the i.r. spectrum corresponds to that of U_3O_8 with two principal bands at 800 cm^{-1} and 740 cm^{-1}. We can therefore identify Stage IV as decomposition of the ammoniate $UO_3 \cdot xNH_3$ represented formally by:

$$3\ (UO_3 \cdot 0.22\ NH_3) = U_3O_8 + \frac{1}{3} N_2 + H_2O \quad \ldots(7)$$

One curious anomaly still remains; as shown in Table 3, the amount of NH_3 retained by the solid prior to Stage IV, is generally too small to account for the stoichiometry of Reaction 7. Apparently stage IV must also involve secondary reactions in which, say, oxides of nitrogen are formed as intermediates, although gas analysis and i.r. data give no direct evidence to support this view. However, TG data indicate that Stage IV is more complex than Reaction 7 implies. Weights of completely self-reduced residues exceed the estimated weight of U_3O_8 by about 0.5 to 1.0 per cent (Figure 12). Excess material is driven off slowly by further heating to give N_2 with some O_2. Most of the gas is evolved between 650°C and 750°C, although some N_2 is still

retained up to 950°C.

3.5 Effect of Atmosphere on Thermal Decomposition of Ammonium Uranate

3.5.1 Decomposition in air

The DTA trace in Figure 12 shows the exothermal peak at 400°C associated with self-reduction in argon. However, AU heated in air exhibits an exotherm at a lower temperature (~ 380°C). This exotherm is due to the reaction of ammoniate $H_3N \rightarrow$ with oxygen from ambient air: at low rates of heating this reaction effectively consumes all retained NH_3 before self-reduction can occur, and the product contains no U(IV); that is, UO_3 is formed. A further endotherm at 650°C denotes the formation of U_3O_8 from UO_3.

At sufficiently high rates of heating, self-reduction temperatures are attained before complete oxidation of ammoniate by oxygen can take place. For example, at a heating rate of 50°C min^{-1}, 27 per cent of uranium in one AU sample (x = 0.39) was reduced to U(IV).

3.5.2 Decomposition in hydrogen

Thermal analysis of AU heated in hydrogen indicates that self-reduction precedes the final reduction to UO_2 by hydrogen gas. The TG and DTA traces in Figure 13 show the self-reduction exotherm at 400°C and a corresponding loss in weight, which is due to formation of U_3O_8. In contrast, the reduction of UO_3 from the parent compound $UO_2(OH)_2$. H_2O is reduced to U_3O_8 at higher temperatures, as indicated by the exothermal peak at 430°C.

3.6 Effect of Nitrate Impurities on Self-Reduction

AU products obtained by precipitation from uranyl nitrate solutions contain ammonium nitrate as a major impurity. The degree of self-reduction is affected markedly by the presence of nitrate, as shown in Table 4.

TABLE 4 - AU PRECIPITATES** HEATED IN ARGON TO 440°C

NH_4NO_3:U	x = NH_4:U* (mole $mole^{-1}$)	Fraction U(IV) in Residue After Heating
0	0.39	0.25
0.05	0.42	0.10
0.19	0.40	0.08
0.21	0.39	0.01

* x refers to NH_4^+ bound in AU i.e. does not include NH_4^+ of ammonium nitrate.

** Prepared by Chemical Engineering Section AAEC RE on pilot plant scale.

Clearly when sufficient NH_4NO_3 is present (about 0.22 mole $mole^{-1}$), self-reduction is completely inhibited. Presumably, before self-reduction can take place, the oxides of nitrogen from NH_4NO_3 oxidise the ammoniate formed in Stage III.

4. REFERENCES

Brown, G. ed. (1961) - X-Ray Identification and Crystal Structure of Clay Minerals. Mineralogical Society, London.

Christ, C.L., Clark, J.R. (1960) - Amer. Minerologist, 44, 1026.

Cordfunke, E.H.P. (1962) - J. Inorg. Nucl. Chem., 24, 303.

Cordfunke, E.H.P. (1970) - J. Inorg. Nucl. Chem., 32, 3129.

Davies, W., Gray, W. (1964) - UKAEA TRG716d.

Dawson, J.K., Wait, E., Alcock, K., Hilton, D.R. (1956) - J. Chem. Soc., 3531.

Ippolitova, E.A., Perchurova, N.I., Gribeink, E.N. (1961) - USAEC Report ANL-TRANS 33, p.114.

Notz, K.J., Mendel, M.G., Huntingdon, C.W., Collopy, T.J. (1960) - USAEC Report TID6228.

Price, G.H. (1971) - J. Inorg. Nucl. Chem., 33, 4085.

Stuart, W.I., Whateley, T.L. (1969) - J. Inorg. Nucl. Chem., 31, 1639.

USAEC (1962) - USAEC Report TID7015, suppl.4.

Woolfrey, J.L. (1969) - AAEC/TM476.

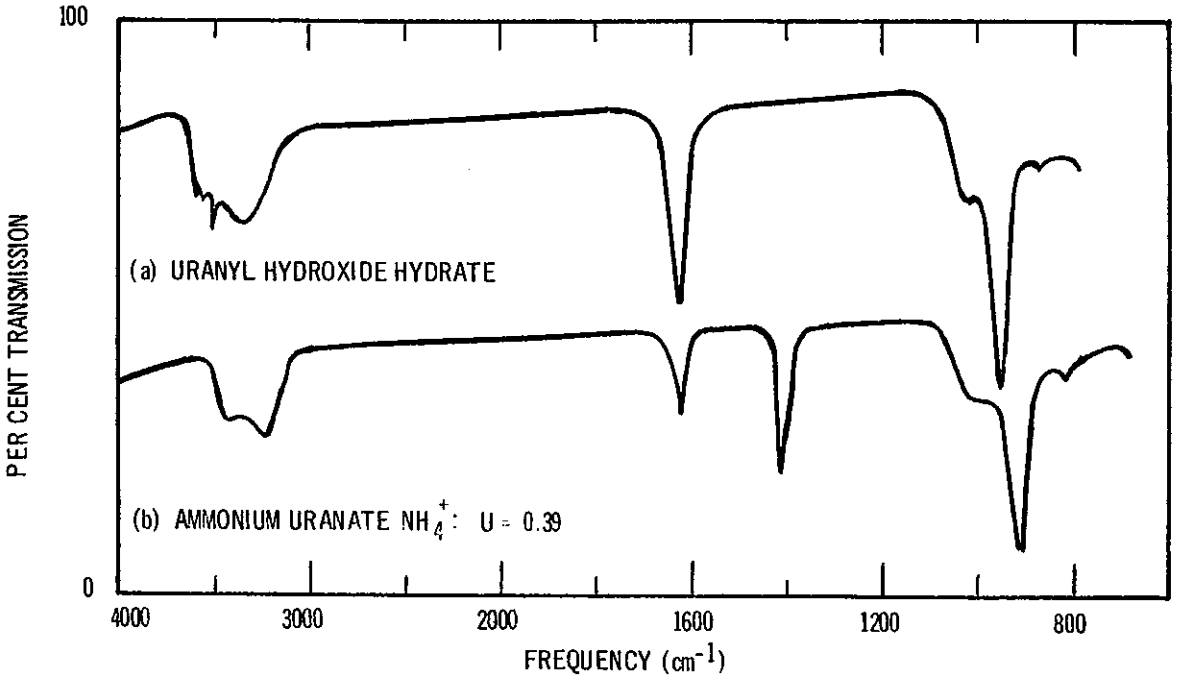

FIGURE 1. INFRA-RED SPECTRUM OF a) URANYL HYDROXIDE HYDRATE AND b) AMMONIUM URANATE

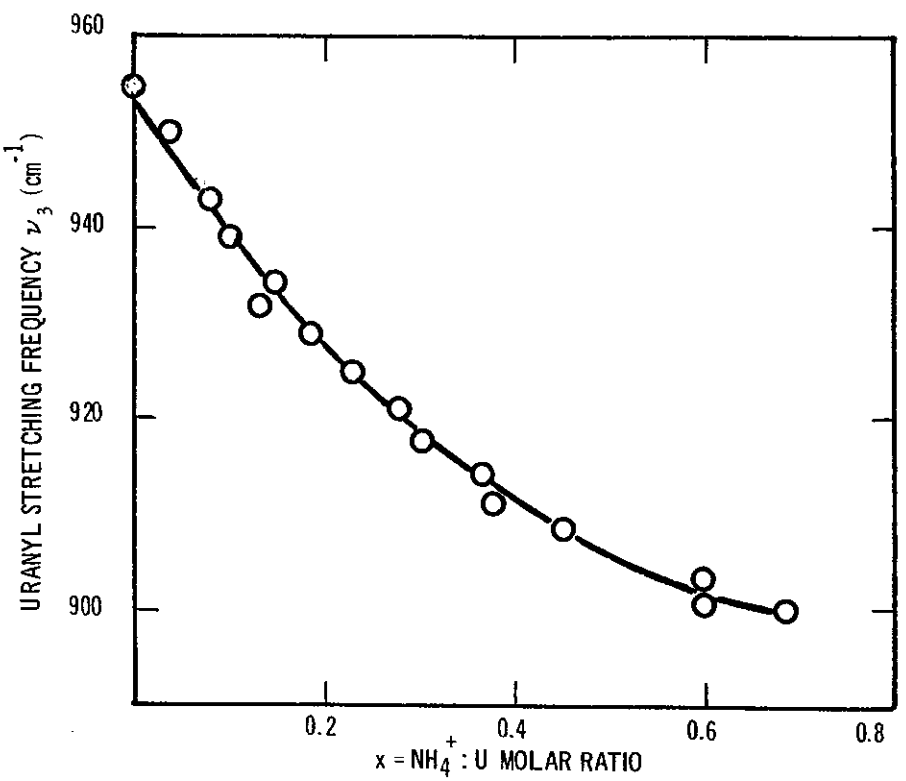

FIGURE 2. VARIATION OF URANYL STRETCHING FREQUENCY ν_3 WITH COMPOSITION OF AMMONIUM URANATE

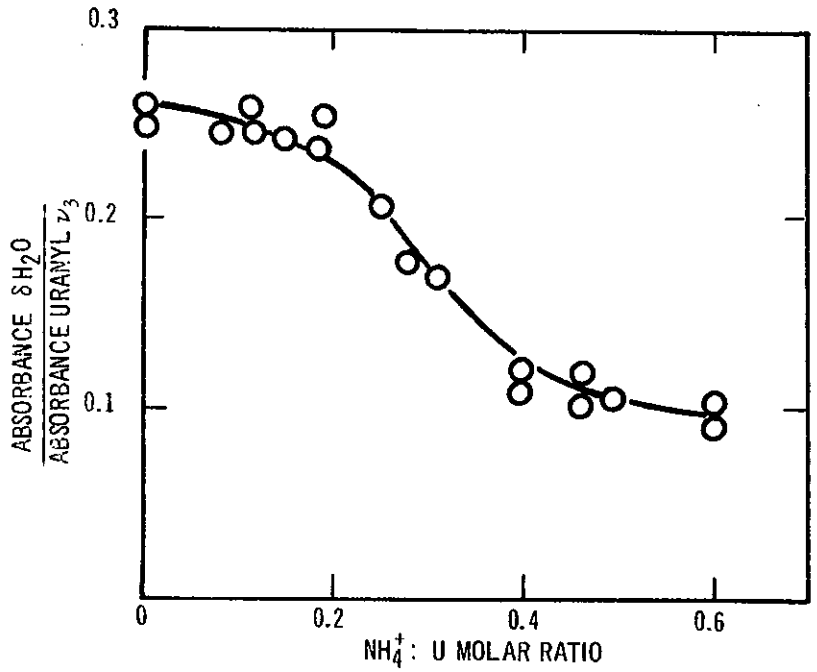

FIGURE 3. VARIATION OF INTENSITY OF H_2O BENDING BAND AT 1620 cm^{-1} WITH COMPOSITION OF AMMONIUM URANATE

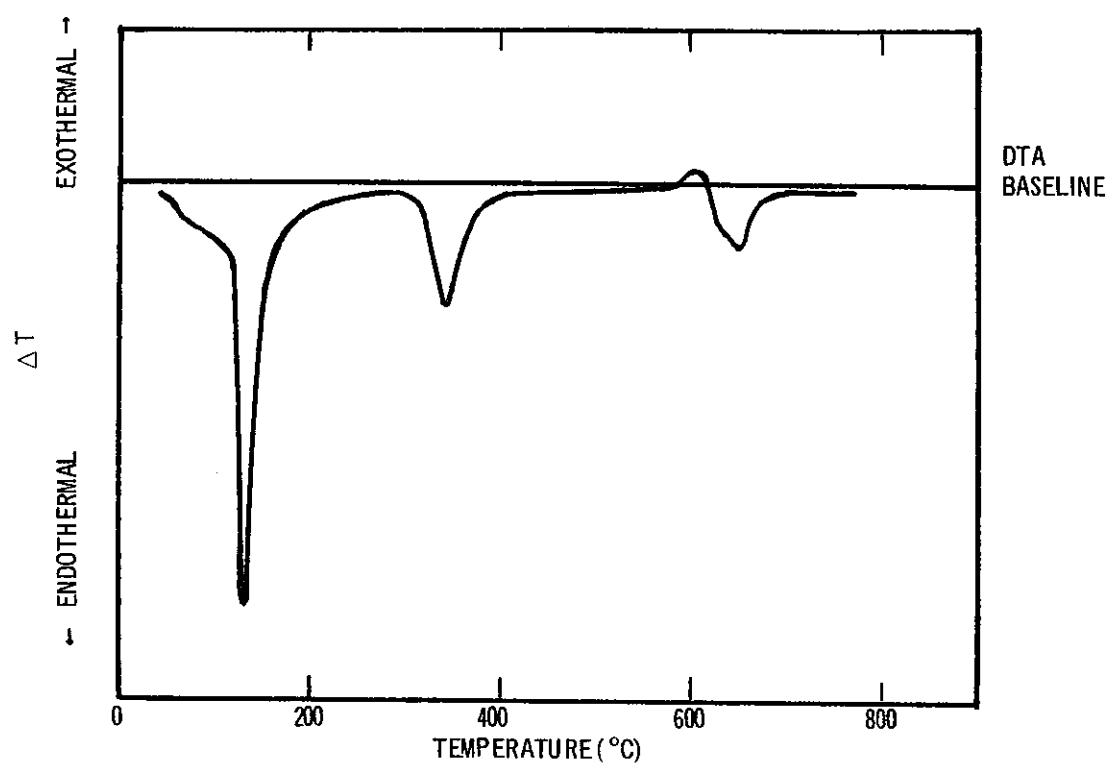

FIGURE 4. DTA TRACE FOR $UO_2(OH)_2.H_2O$ HEATED IN NITROGEN AT 5°C min^{-1}

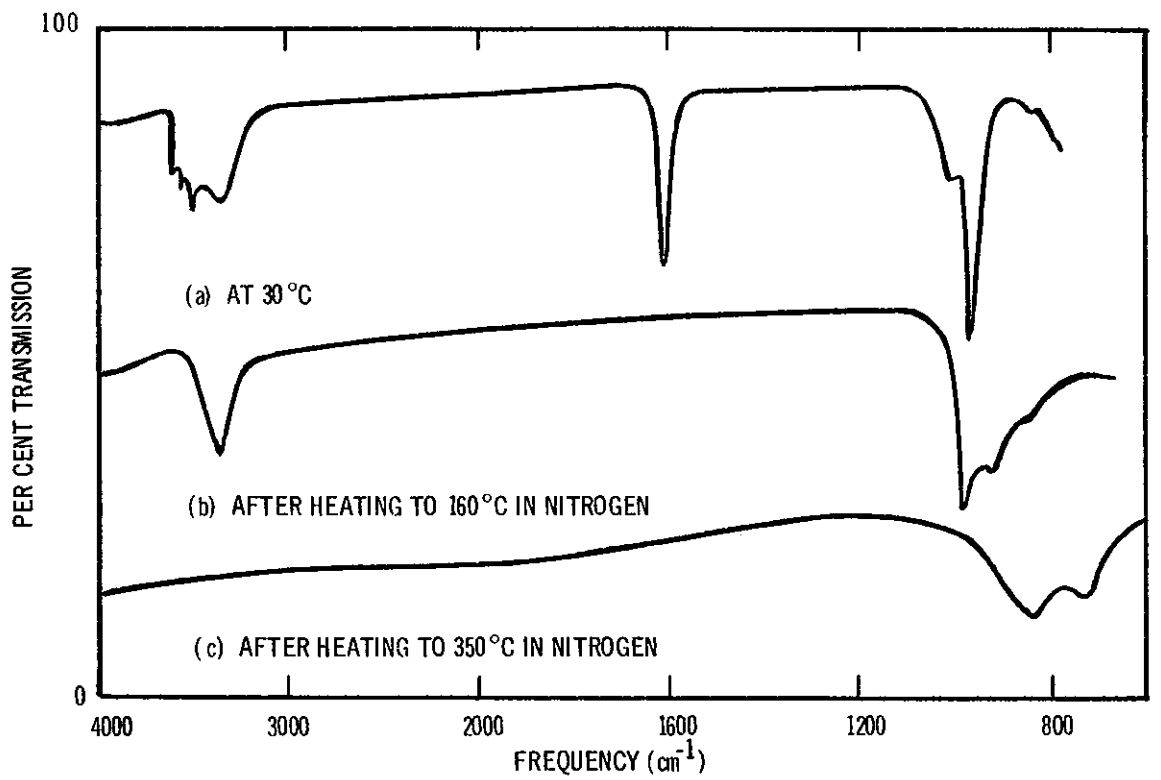

FIGURE 5. INFRA-RED SPECTRUM OF URANYL HYDROXIDE HYDRATE a) AT 30°C b) AFTER HEATING TO 160°C IN NITROGEN AND c) AFTER HEATING TO 350°C IN NITROGEN

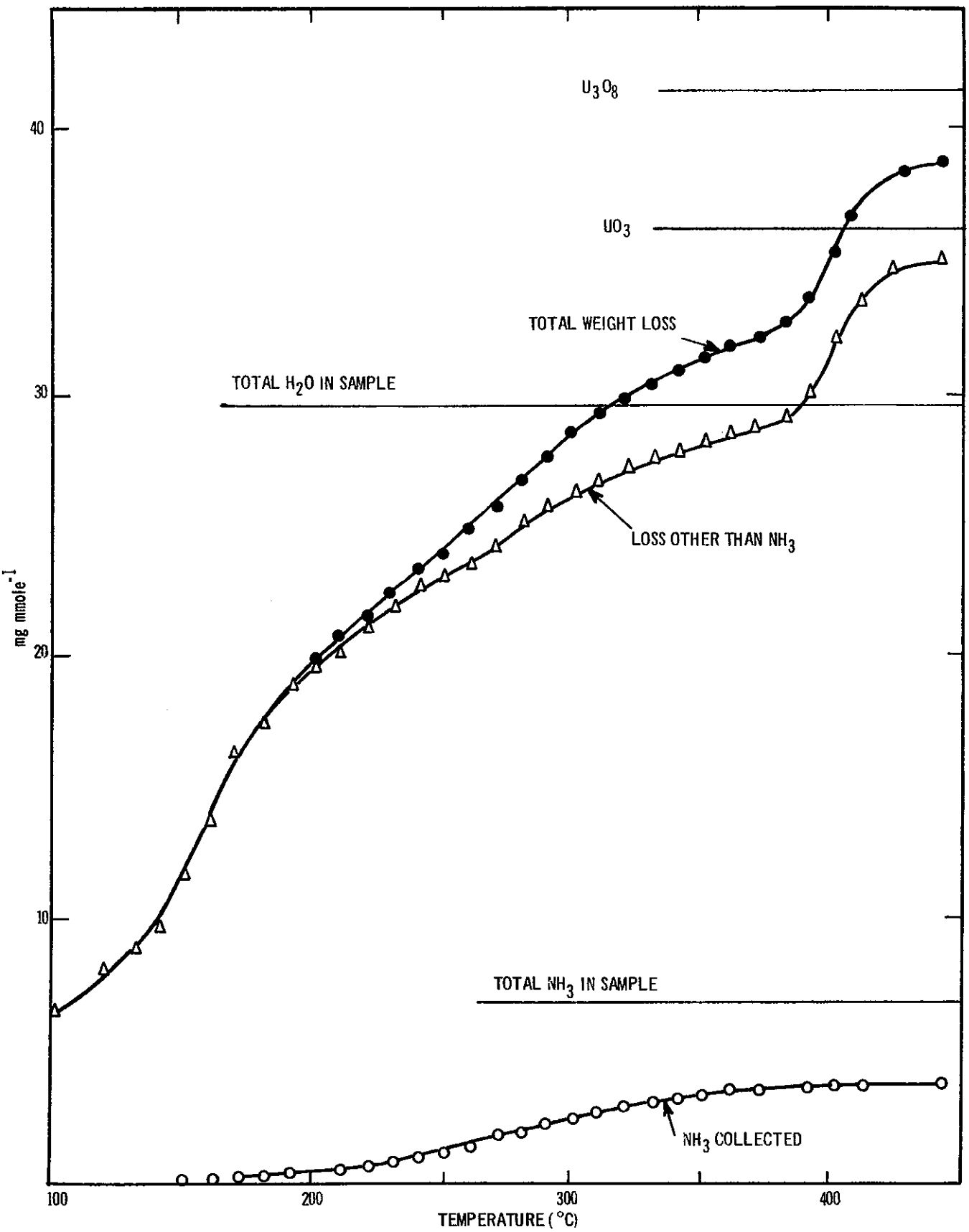

FIGURE 6. THERMOGRAVIMETRIC (TG) DATA FOR AMMONIUM URANATE (NH_4^+ : U = 0.39) HEATED IN ARGON AT 5°C min^{-1}

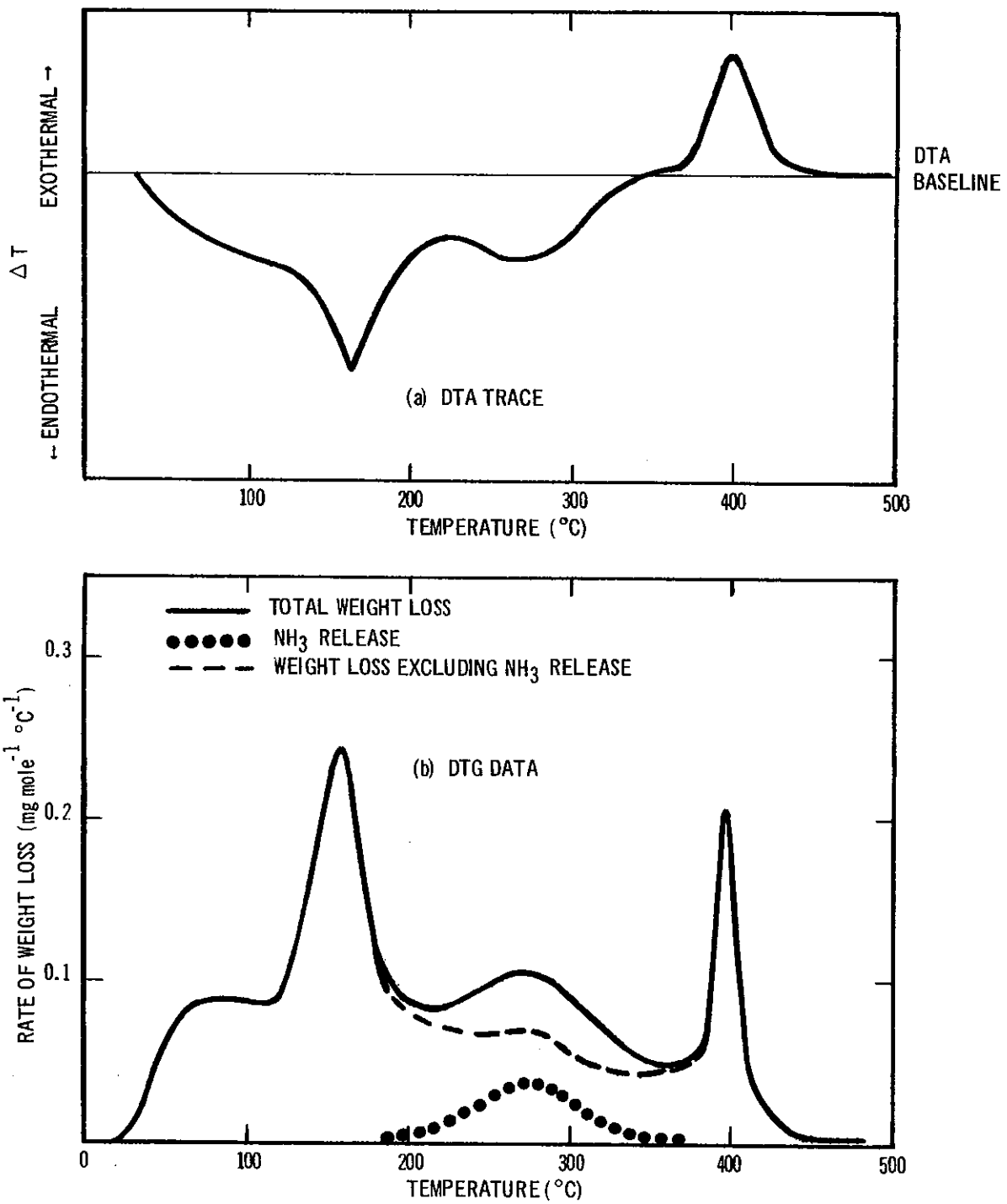

FIGURE 7. THERMOANALYTICAL DATA FOR AMMONIUM URANATE (NH_4^+: U = 0.39) HEATED IN ARGON AT 5°C min^{-1} a) DTA TRACE, b) DIFFERENTIAL THERMOGRAVIMETRIC (DTG) DATA

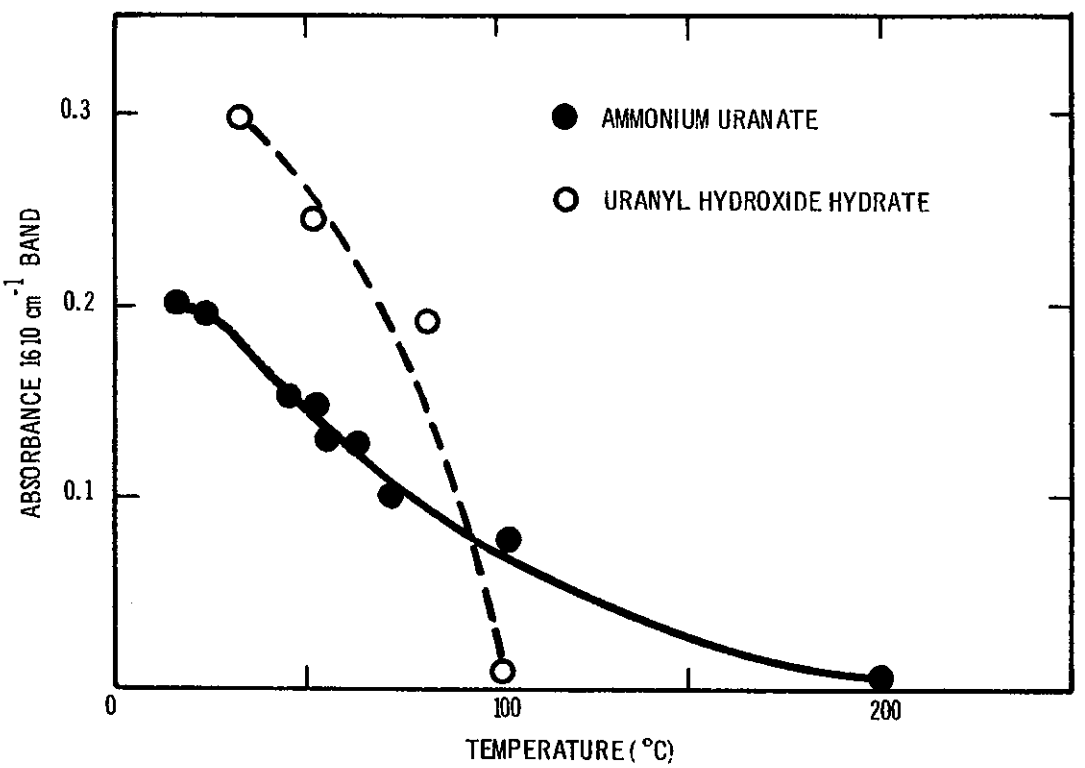

FIGURE 8. VARIATION WITH TEMPERATURE OF δH_2O BAND OF COORDINATED WATER MOLECULES IN AU(NH_4^+: U = 0.4) AND URANYL HYDROXIDE HYDRATE. SOLIDS HEATED TO 200°C IN A SERIES OF 3-4 min ISOTHERMAL ARRESTS

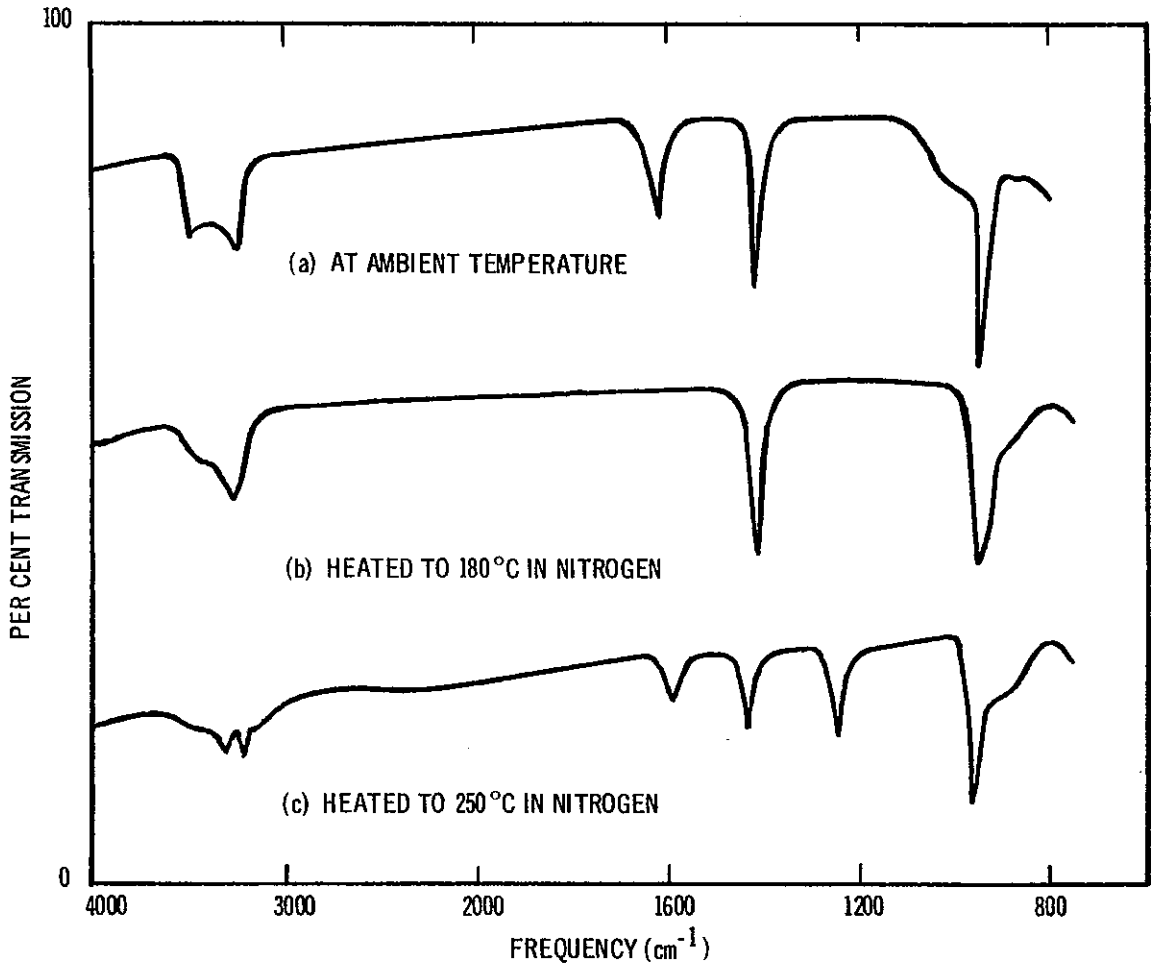

FIGURE 9. INFRA-RED SPECTRUM OF AMMONIUM URANATE a) AT AMBIENT TEMPERATURE b) HEATED TO 180°C IN NITROGEN AND c) HEATED TO 250°C IN NITROGEN

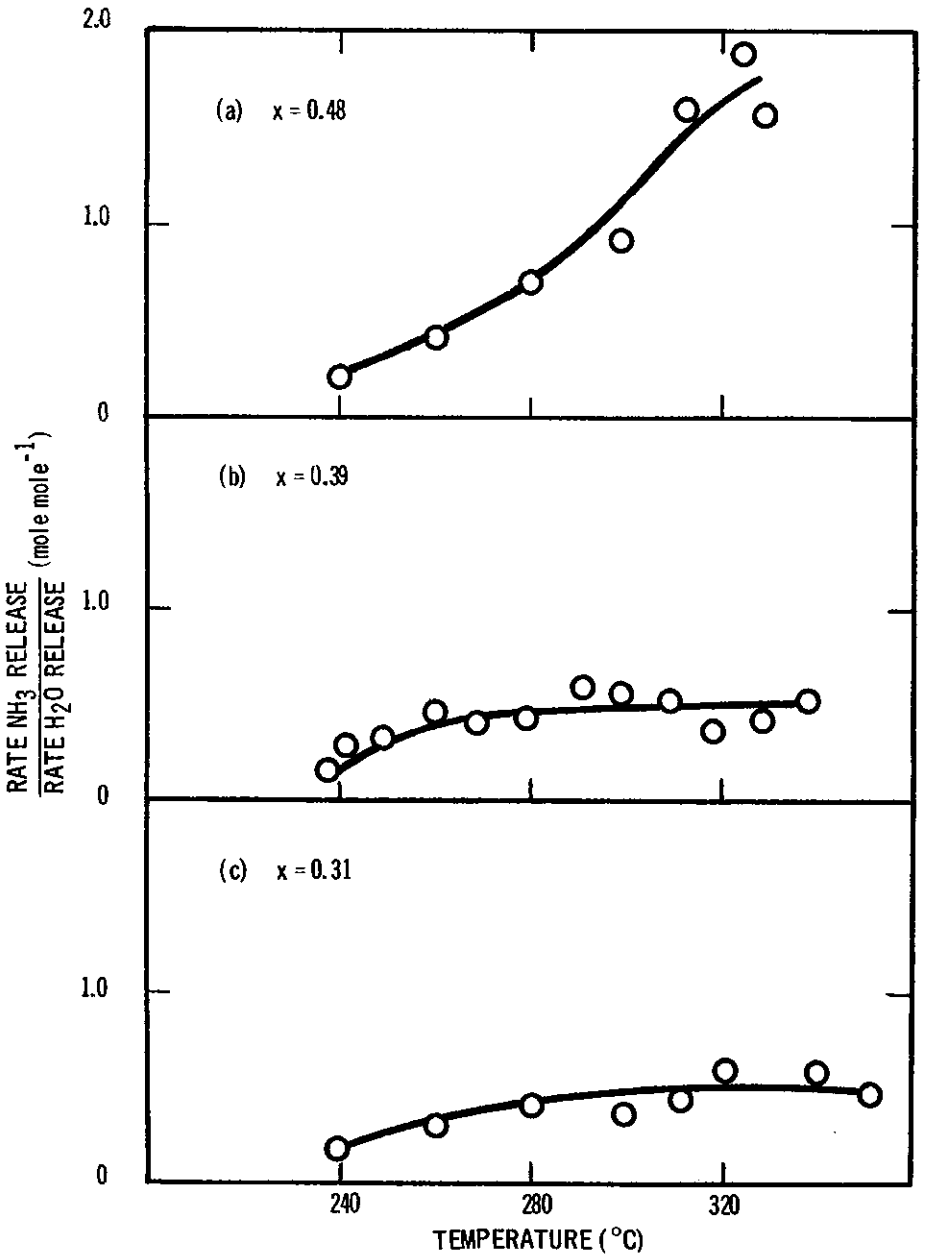

FIGURE 10. AMMONIUM URANATES HEATED IN ARGON AT 5 °C min^{-1}. EVOLUTION OF NH_3 AND H_2O IN STAGE III DECOMPOSITION

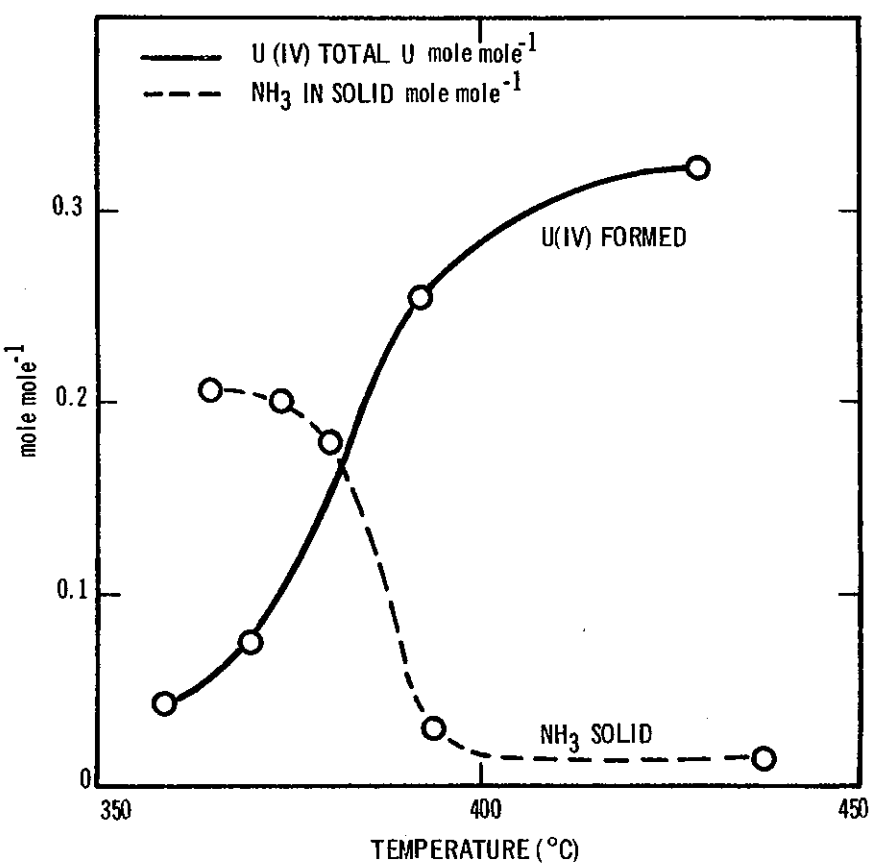

FIGURE 11. AMMONIUM URANATE (x = 0.38) HEATED IN ARGON AT 5°C min^{-1}, STAGE IV.

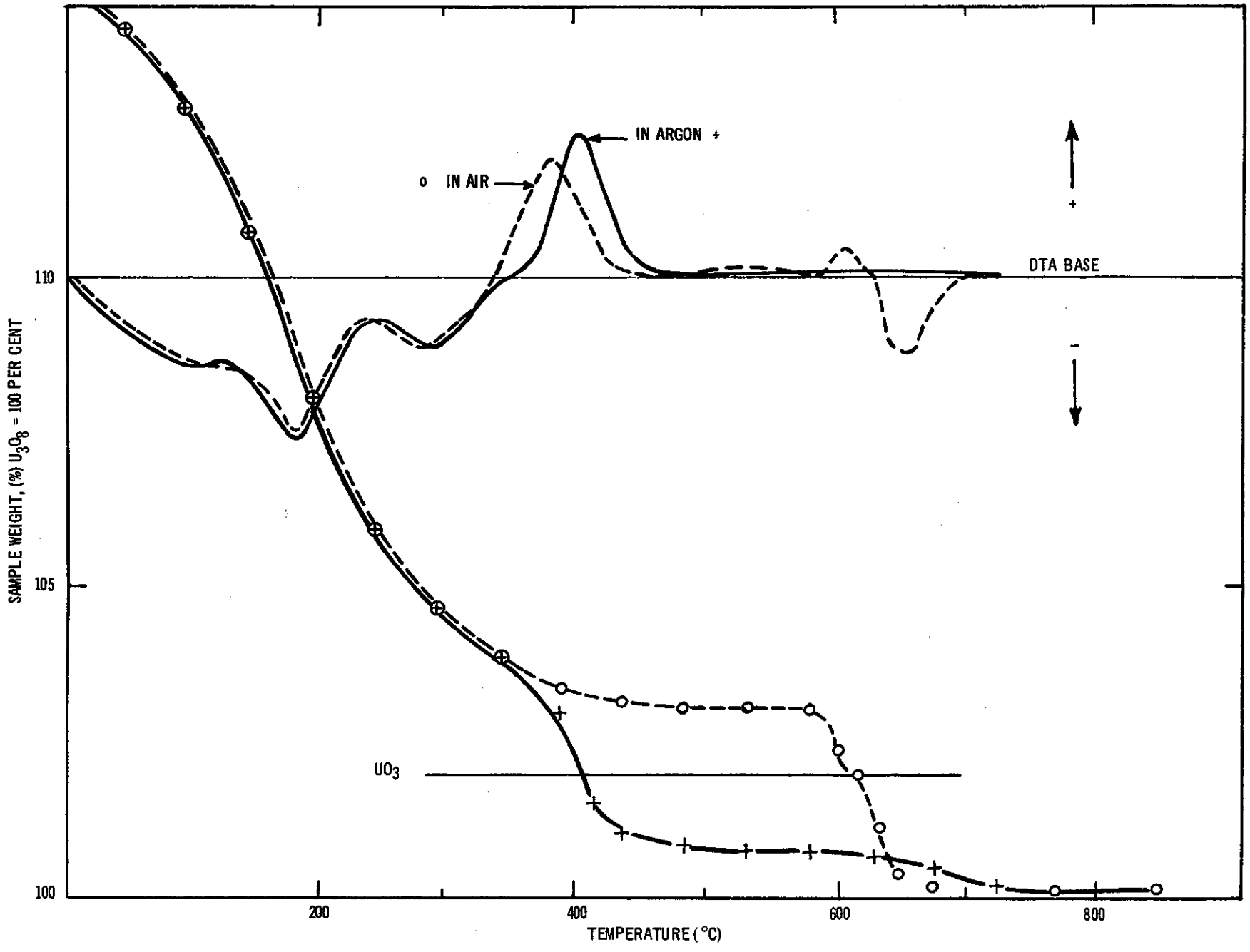

FIGURE 12. DTA AND TG TRACES FOR AMMONIUM URANATE HEATED IN ARGON AND DRY AIR AT 5°C min-1

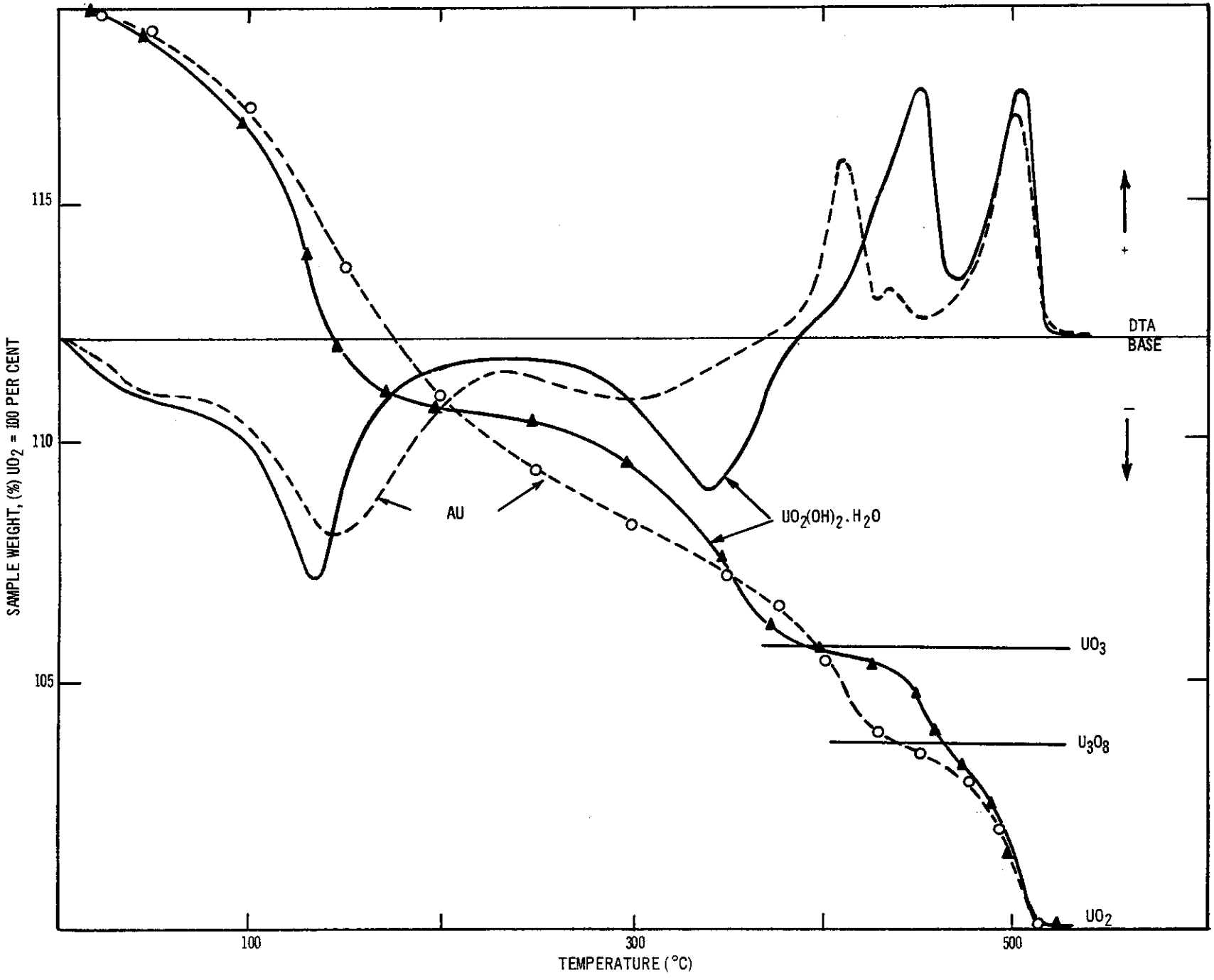

FIGURE 13. DTA AND TG TRACES FOR $UO_2(OH)_2H_2O$ AND AMMONIUM URANATE HEATED IN HYDROGEN AT 5°C min^{-1}

APPENDIX

THE NATURE OF AMMONIUM URANATES

According to Cordfunke (1962) the ammonium uranate (AU) system embodies four distinct compounds designated

$I = UO_3 \cdot 2H_2O$, $II = UO_3 \cdot 0.33\ NH_3 \cdot 1.67\ H_2O$

$III = UO_3 \cdot 0.5NH_3 \cdot 1.5H_2O$ and $IV = UO_3 \cdot 0.67NH_3 \cdot 1.33H_2O$

with intermediate compositions representing two-phase mixtures of (I + II), (II + III) etc. In contrast, the results of Stuart and Whateley (1968) indicate a continuous AU system described by $UO_2(OH)_{2-x}\ (ONH_4)_x yH_2O$ where x varies continuously in the limits x = 0 to x ~ 0.7.

Recently Cordfunke (1970) suggested that AU samples prepared from $UO_3 \cdot 2H_2O$ (uranyl hydroxide hydrate, $UO_2(OH)_2 \cdot H_2O$) by Stuart and Whateley were non-equilibrium products. In proposing this explanation he stated that results obtained using anhydrous UO_3 'wholly confirmed previous results' (that is, confirmed the multiphase hypothesis). It is not clear that experiments using $UO_3 \cdot 2H_2O$ provided similar confirmation even after reaction periods of 18 weeks. Also he did not provide definitive evidence to distinguish between equilibrium and non-equilibrium states.

To clarify these matters we have further studied AU formation using both $UO_3 \cdot 2H_2O$ and anhydrous UO_3 as starting materials.

1. REACTION OF $UO_3 \cdot 2H_2O$ WITH NH_4OH SOLUTION AND NH_3 GAS

Samples of $UO_3 \cdot 2H_2O$ were reacted with various amounts of NH_4OH solution or NH_3 for at least 26 weeks. The resulting AU products were examined using i.r. spectrophotometry and X-ray diffraction techniques. Our results have the same features as those of Stuart and Whateley: each product shows only a single absorption band assigned to the asymmetric uranyl stretching frequency ν_3, and ν_3 decreases continuously from 955 cm^{-1} for $UO_3 \cdot 2H_2O$ to about 890 cm^{-1} for NH_3: U = 0.7. Changes in composition induce detectable changes in structure, but as reported previously (Stuart and Whateley 1969) X-ray diffraction patterns do not relate to X-ray data of synthetic two-phase mixtures. This is particularly evident for the composition range NH_3: U < 0.12: in this range, X-ray diffraction patterns are similar to that of $UO_3 \cdot 2H_2O$, but lattice dimensions vary continuously with composition (for example, an increase of about 1.2 per cent in the c axis and 0.8 per cent in the a and b axis is apparent for NH_3: U = 0.12).

Thus AU samples prepared from $UO_3 \cdot 2H_2O$ have the properties of a

continuous system even after long reaction times. To determine whether or not this continuous system represents equilibrium it is then necessary to define 'non-equilibrium products'. Consider, for example, a reaction of $UO_3 \cdot 2H_2O$ and NH_4OH leading to a product with NH_3: U ratio less than 0.33, say 0.2. If the multiphase hypothesis is correct, this reaction should then lead to an equilibrium mixture of Type I ($UO_3 \cdot 2H_2O$) and Type II compounds, and a non-equilibrium state could arise through two effects. These are:

(i) Incomplete reaction of $UO_3 \cdot 2H_2O$. In this instance i.r. data would show two absorptions at 955 cm^{-1} and about 915 cm^{-1} corresponding respectively to Type I and Type II phases. However, this is not the case for our AU products prepared from $UO_3 \cdot 2H_2O$.

(ii) Alternatively a non-equilibrium product could be a metastable single phase of uniform composition which slowly disproportionates to form an equilibrium two-phase mixture thus:

$$UO_3 \cdot 2H_2O \xrightarrow{NH_4OH} \underset{\text{metastable single phase}}{UO_3 \cdot 0.2NH_3 \cdot yH_2O} \rightarrow$$

$$\text{disproportionation} \rightarrow \underset{\text{Type I}}{0.39\,[UO_3 \cdot 2H_2O]} + \underset{\text{Type II}}{0.61\,[UO_3 \cdot 0.33NH_3 \cdot 1.67H_2O]} \quad \ldots(1)$$

with the metastable intermediate showing a single uranyl absorption band.

To test the feasibility of the reaction scheme given by Equation (1) we prepared various mixtures of AU (NH_3: U = 0.33) and $UO_3 \cdot 2H_2O$. Portions of each mixture were ground in both nujol and ethanol. Results of X-ray and i.r. measurements indicate that grinding in ethanol induces a reaction between AU and $UO_3 \cdot 2H_2O$ to form a uniform single phase. For example, a mixture with a mean ratio NH_3: U = 0.12 prepared as a nujol mull shows two distinct bands at 955 cm^{-1} and 916 cm^{-1} as one might expect from a two-phase mixture. A similar mixture after grinding for a few seconds in ethanol also shows band splitting and the X-ray diffraction pattern is a composite of the two components; but after further grinding in ethanol only a single uranyl band at 936 cm^{-1} can be observed and the X-ray diffraction pattern qualitatively resembles that of $UO_3 \cdot 2H_2O$ although some lattice expansion is evident.

Similar reactions can be induced by adding $UO_3 \cdot 2H_2O$ to a slurry of AU and parent NH_4OH solution and then grinding the mixture for 48 hours in a sealed container. Other AU products with higher NH_3: U ratios when mixed together in ethanol in a variety of combinations also react to form a uniform single phase.

It is difficult therefore to accept the notion of a reaction scheme represented by Equation (1). Our results indicate the contrary; that a two-phase mixture is a metastable system which reacts in favourable conditions to form a uniform single phase. We conclude therefore that the multiphase hypothesis is not correct.

2. REACTION OF ANHYDROUS UO_3 WITH NH_4OH SOLUTION

The reaction of anhydrous UO_3 and NH_4OH is complicated by competing processes of hydration and ammoniation. It is then probable that the evidence supporting the multiphase hypothesis (evidence derived from the reaction of anhydrous UO_3) in fact arises from complex kinetic effects leading to metastable non-uniform products.

Our experimental evidence supports this view. After comparing the reactions of UO_3 with liquid water and NH_4OH solutions, we find that hydration of UO_3 is inhibited in NH_4OH solution, by the competing ammoniation process.

More notably, rates of hydration in NH_4OH depend upon particle size, with larger particles hydrating the more slowly. In contrast the larger particles absorb NH_4^+ preferentially.

Referring specifically to the UO_3 used by us, each final AU product could be divided roughly into two fractions: a 'heavy' fraction of larger particles which settled immediately after shaking in NH_4OH solution and a 'light' fraction which settled after a longer time. The two fractions of each AU product showed distinct differences in colour and composition. In each case the NH_3: U ratio was greater for the larger particles and the frequency ν_3 was correspondingly lower. Chemical uniformity as indicated by merging of uranyl absorption bands and changes in X-ray diffraction pattern could usually be achieved by grinding in ethanol.

These observations refer of course to a particular batch of powder and clearly kinetics of reaction must depend upon particle size distribution and powder morphology. But a general conclusion seems valid, that the reaction frequently leads to metastable, chemically non-uniform products; and this is a consequence of particle-size distribution. Slow hydration of larger particles allows preferential absorption of NH_4^+, whereas competing processes of hydration and ammoniation lead to lower NH_3: U ratios of the smaller particles.

We conclude finally that the AU system at equilibrium is a continuous non-stoichiometric system with zeolite-type properties. This is as one might expect from the cation-exchange properties of $UO_3 \cdot 2H_2O$ (uranyl hydroxide hydrate) since ion-exchange by definition implies non-stoichiometry.